Geopersia ***9*** *(1), 2019, PP. 89-109* *DOI: 10.22059/GEOPE.2018.257280.648387*

Microfacies, geochemical characters and possible mechanism of rhythmic deposition of the Pabdeh Formation in SE Ilam (SW Iran)

Zahra Hosseini Asgarabadi[1], Saeed Khodabakhsh[1*], Hassan Mohseni[1], Galen Halverson[2], Thi Hao Bui[2], Nasrollah Abbassi[3], Abdol–Reza Moghaddasi[4]

[1] Department of Geology, Faculty of Sciences, Bu–Ali Sina University, Hamadan, Iran

[2] Department of Earth and Planetary Sciences, McGill University, Montr´eal, Canada, QC H3A0E8

[3] Department of Geology, Faculty of Sciences, University of Zanjan, Zanjan, Iran

[4]Exploration directorate of National Iranian Oil Company, Iran

**Corresponding author, e–mail: saeed@basu.ac.ir*

(*received: 07/05/2018 ; accepted: 27/10/2018*)

Abstract

Rhythmical alternations between limestone and marls characterize the Pabdeh Formation (Paleocene–Oligocene), in Zagros basin, south–west Iran. Using petrography (microfacies analysis and SEM investigation) and geochemical parameters (elemental, XRD and stable ^{13}C and ^{18}O isotopes) analysis, three intervals of limestone/marl alternations in one exposed section were studied to unravel the possible mechanisms responsible for the origin of these rhythmites. Microfacies study shows alternation of carbonate microfacies (mudstone and wackestone) with marl lithofacies. The microfacies analysis reflects calm deep–water sedimentation that was interrupted by sporadic traction currents from shallow–marine. Evidence such as mixed broken and oriented shallow–marine bioclasts, detrital quartz grains with planktonic foraminifera and micritic matrix imply the traction currents, responsible for detrital transport from shallow–marine to deep–marine. The content of TiO_2, SiO_2 and Al_2O_3 (obtained from the element composition analysis) shows the difference between limestones and marls in interval 1, each following an individual trend line indicating a bimodal chemical composition and varying delivery mechanisms. However, for the intervals 2 and 3, there is no significant difference in the trend lines. The oxygen isotope signature of samples is between –5.68 to –1.01‰ and the carbon isotope signature is between –3.53 to +0.73‰. The isotope data ($\delta^{18}O$ and $\delta^{13}C$) for limestones and marl rhythms compared with Eocene marine calcite show post depositional alteration. Limestone–marl alternations in the interval 1, therefore, originated from the cyclic changes in siliciclastic input by shallow–water derived currents (probably turbidity currents; *sensu* Mohseni *et al.,* 2011). However, for the intervals 2 and 3, although the field observations (such as extensive lateral continuity of individual beds and sharp contact between different lithologies) and some of the petrography parameters such as existence of the microfossils with similar preservation quality suggest the primary rhythm as a major mechanism, whereas the geochemical data do not strongly support this conclusion.

Keywords: *Pabdeh Formation, Stable Oxygen and Carbon Isotope, Zagros Basin, Limestone–Marl Alternations.*

Introduction

Limestone–marl/shale alternations are known from deposits of all Phanerozoic ages such as limestone–shale/marl alternations of Lower Lias of SW Britain (Arzani, 2004, 2006), Upper Cretaceous pelagic and hemipelagic limestone– marl alternations of Zumaya in northern Spain, (Mount & Ward, 1986) and Cretaceous pelagic limestone–marl alternations Blake–Bahama Basin (Westphal *et al*., 2004). The alternations abundance varies strongly in different geologic periods (Westphal *et al*., 2008). Their abundance follows the oscillations between calcite versus aragonite seas with high abundances during the times of calcite seas and less abundance during times of aragonite seas (Biernacka *et al.,* 2005; Colombie *et al*., 2012; Collart, 2013). Limestone–marl/shale alternations are characterized by their conspicuous appearance in outcrop with a pronounced ABAB pattern (regular repetition of two different lithologies) rhythm of more weathering–resistant limestone beds versus softer counterparts (marl/shale beds). These alternations have been interpreted as reflecting cyclic depositional changes or, conversely, being solely of diagenetic origin (acting on homogeneous sediment) (Biernacka *et al.,* 2005; Arzani, 2006; Colombie *et al.,* 2012). The former interpretation assumes that each individual layer carries an environmental signal and—as a whole—the section is considered as a geological record of temporal environmental changes, such as orbitally forced climatic fluctuations. All of these examples concerned deep–water sediments. Four main types of mechanisms forming pelagic calcareous rhythmites have been recognized (Biernacka *et al.,* 2005; Colombie *et al.,* 2012; Eldrett *et al.,* 2015): (a) productivity cycles reflecting a variable supply of biogenic carbonate, (b) dilution cycles predicated upon periodic fluctuation of supply of fine terrigenous sediments, (c) dissolution cycles related

to periodic dissolution of carbonate and (d) calcareous redox cycles indicating fluctuations of bottom water oxygenation. The role of diagenesis in these "depositional models" has not been ignored, although it has been assumed that the environmental signal is not entirely blurred by subsequent modification (Biernacka *et al.,* 2005). Opposing these models, diagenetic scenarios describe limestone–marl couplets as products of homogenous or nearly homogenous precursor sediment (Munnecke & Samtleben, 1996; Munnecke *et al.,* 1997; Arzani, 2006). This hypothesis has been postulated on the basis of differential diagenesis between limestone and marl layers: limestones usually undergoing cementation during early diagenesis, whereas marls were subject to dissolution processes. Frequently, limestone layers contain well preserved delicate fossils and undeformed or only slightly deformed trace fossils; whereas in marls, fossils are flattened, deformed or even dissolved away. The calcium carbonate necessary to cement limestone layers was believed to be derived from dissolution of calcite in adjacent marls (Munnecke *et al.,* 1997; Westphal *et al.,* 2000; Arzani, 2006). Owing to these diagenetic modifications, an interpretation of sediment properties in terms of environmental fluctuations is often difficult. Hence, for interpretation of origin of a rhythmic calcareous succession, some parameters are needed which are either diagenetically inert or assessable in terms of the diagenetic difference (Westphal *et al.,* 2008). The contribution of event deposits (tempestite/turbidites) to various basin fills can be very significant, higher than 90% in some cases. Events may lead to the formation of limestone–marl/shale alternations, which can also result from cyclic changes in sea level or climate (Colombie *et al.,* 2012). Khodabakhsh *et al.,* (2009) studied the significance of event deposits in the study area (NE Ilam, Zagros Basin). Lithologically, the Pabdeh Formation consists of argillaceous limestone, shale and marl and have two members, Purple shale Member and Taleh Zang Member (Motiei, 1993). During the Paleocene and Eocene, the pelagic marls and argillaceous limestones of the Pabdeh Formation were deposited in the middle part of the Zagros basin (Motiei, 1993), in a ramp environment (somehow in intrashelf basin, Mohseni *et al.,* (2011). Such basins (due to events) are commonly suitable for deposition of rhythmically bedded strata (Eldrett *et al.,* 2015). Paleocene–Oligocene sequence paleogeography on the Arabian plate shows that the Zagros foreland basin subsided since late Cretaceous until early Eocene and the Pabdeh Formation was deposited within the foredeep setting (Zeigler, 2001). During the middle–late Eocene, the sea level gradually fell and the Zagros foredeep along with the sediment package almost remained unchanged. In the central part of the foredeep, sedimentation continued with silty to sandy shales alternating with argillaceous limestone intercalations which is totally similar to the Pabdeh Formation. The pronounced fall in sea level during the Oligocene the entire Arabian Plate exhumed. The Neo–Tethys ceased rapidly and the Zagros foredeep became a narrow trench in which carbonate dominated sucession were deposited along its margins. (Zeigler, 2001). The Paleocene–Eocene is episode of global warming and sea level rise (Sluijs *et al.,* 2014). Khavari *et al.,* (2014) proposed the oligotrophic conditions during the Paleogene and the mesotrophic–eutrophic conditions during the Oligocene based on nanofossil content of the Pabdeh Formation in south west of Iran (Ilam section). Based on calcareous nannofossils of the Pabdeh Formation in Khoozestan Province, Senemari (2018) put forward oligotrophic conditions and tropical climate for the lower part and temperate climate for the upper part of the Pabdeh Formation.

The Pabdeh Formation as an oil source and/or reservoir rock of the Zagros basin was well appreciated by geologists; rhythmic alternations characterize parts of the Pabdeh Formation in Southwest of Iran; the origin of the rhythmic alternations yet unravel. The main objective behind the present research is to figure out the possible mechanisms responsible for the origin of these rhythmites in the study area and examining primary versus diagenetic origin of them. For this purpose a multi–proxy approach was used to study the Pabdeh Formation in Northwest of the Zagros basin (Southeast of Ilam).

Geological setting and stratigraphy

The study area is located in the Zagros basin which comprises 7–14 km thick sedimentary succession that covers its Precambrian basement (Alavi, 2004). The Zagros basin has evolved through a number of different tectonic settings since the end of Precambrian. The basin was a part of the Gondwana supercontinent in Paleozoic, a passive margin in Mesozoic, and became a convergent orogen in Cenozoic (Bahroud & Koyi, 2004; Sepehr &

Cosgrove, 2004). Since late Triassic, the Neo–Tethys Ocean were developed between Arabia and Iran. The closure of the Neo–Tethys, mostly during the Oligocene was due to subduction of the Arabian plate beneath the Iranian sub–plate (Berberian & King, 1981; Stoneley, 1981; Berberian, 1995). During Cenozoic continent–continent collision led to the formation of the Zagros fold–and–thrust belt (ZFTB), which brought the Zagros foreland basin where has continually delivered sediments since Late Cretaceous to Miocene. The sedimentary sequence include the Gurpi Formation (marl and shale), the Amiran Formation (siltstone, sandstone, limestone and conglomerate), the Pabedeh Formation (argilaceous limestone, marl and shale), the Taleh Zang Formation (limestone), the Kashkan Formation (siltestone, sandstone and conglomerate), the Shahbazan Formation (dolomite limestone and dolomite), the Asmari Formation (limestone), the Gachsaran Formation (anhydrite, marl and limestone) and the Agha Jari Formation (calcareous sandstone, siltstone and sandstone) (James & Wynd, 1965). The Pabdeh Formation in the type section (Tang–e Pabdeh) (Fig. 1, A), is 798m thick, and consists of shale and thin–bedded clayey limestones. Its lower contact is distinguished from the Gurpi Formation (upper Cretaceous) by the Purple Shale Member and the upper contact is gradational and conformable with the Asmari Formation. The Pabdeh Formation extends in the majority of the Zagros basin including Fars, Khozestan and Lorestan (Mirzaee – Mahmoodabadi *et al.,* 2010) (Fig. 1, B).

Study area

The sedimentary succession studied here (the Gandab surface section) belongs to the Pabdeh Formation, situated in the Northwest of the Zagros basin.

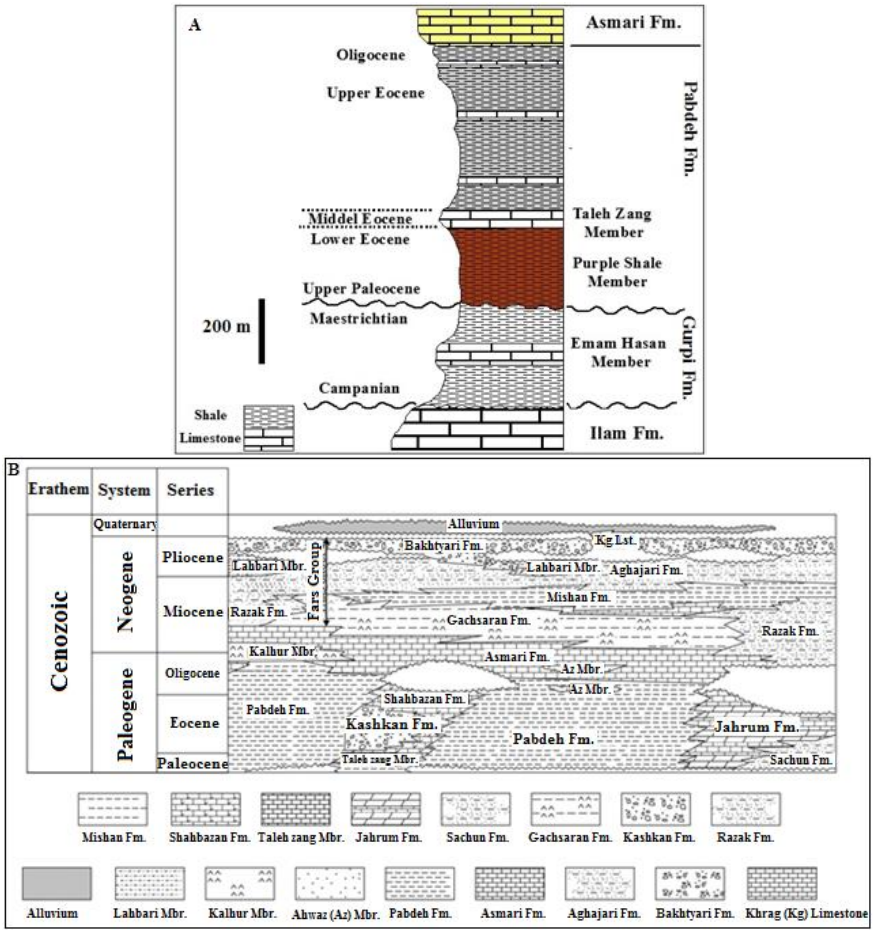

Figure 1. Simplified stratigraphic chart; A: of the type section of Pabdeh Formation; B: of the Cenozoic of the Zagros basin (modified after James and Wynd, 1965).

This basin was a part of the southern margin of Neo–Tethys Ocean (Alavi, 2004) filled by terrigenous and carbonate sediments. The Gandab section is located in southeast of the Ilam Province (Fig. 2). Its lower boundary is identified from Gurpi Formation by the Purple Shale Member and the upper contact with the Asmari Formation (Fig.3) is marked by an evaporitic horizon. Total thickness of the section is about 330m. The succession includes four rock units: purple shale, bioturbated argillaceous limestone, calcareous marl and marl. In some parts of this section, rhythmic alternations between argillaceous limestone – marl and calcareous marl–marl are visible of which three intervals are more pronounced and distinguishable. These intervals are (interval 1: 6.46m, from the lower part; interval 2: 1m from the mid part and interval 3: 11.25m, from the upper part of the Pabdeh Formation) (Fig. 4). In the interval 1, alternation is between limestone (argillaceous limestone) and marl, in the interval 2, is between calcareous marl and marl; while the interval 3, is almost between argillaceous limestone and marl. In this study, calcareous marl, marl and argillaceous limestone are referred to the carbonate content which include 65 –75%, 35–65% and 75 – 95% $CaCO_3$, after Pettijhon *et al.,* 1975 respectively.

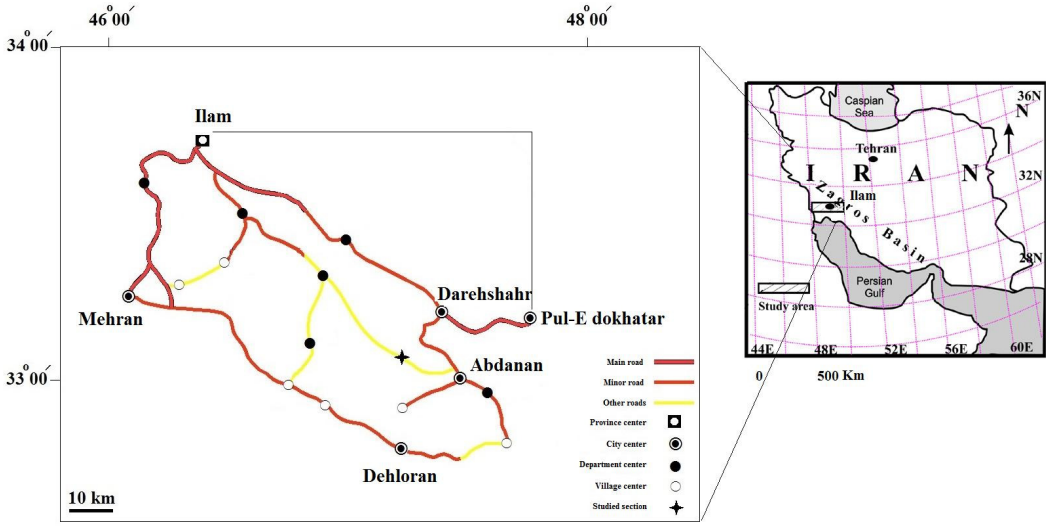

Figure 2. Location map of the studied section.

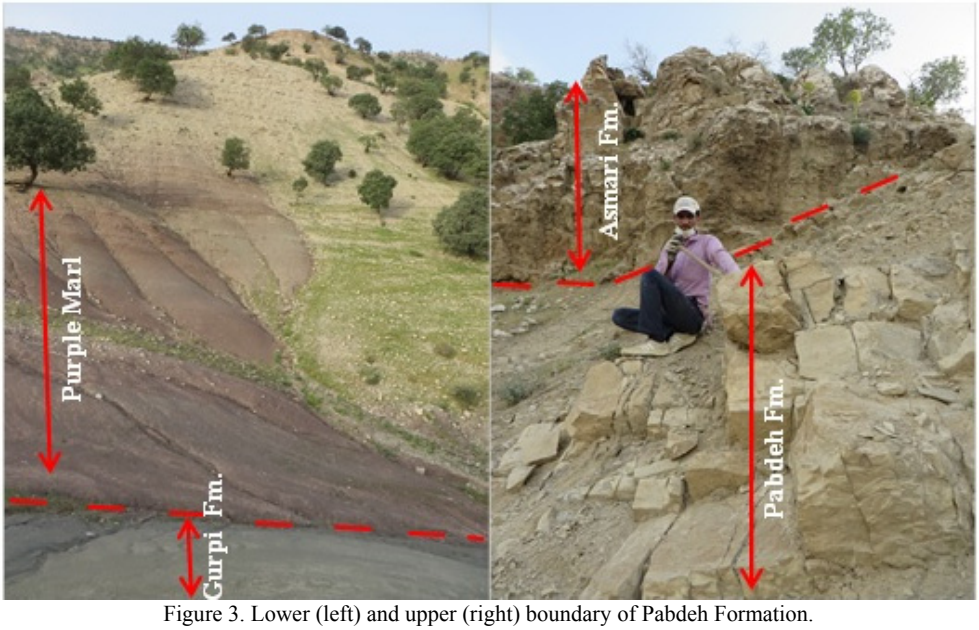

Figure 3. Lower (left) and upper (right) boundary of Pabdeh Formation.

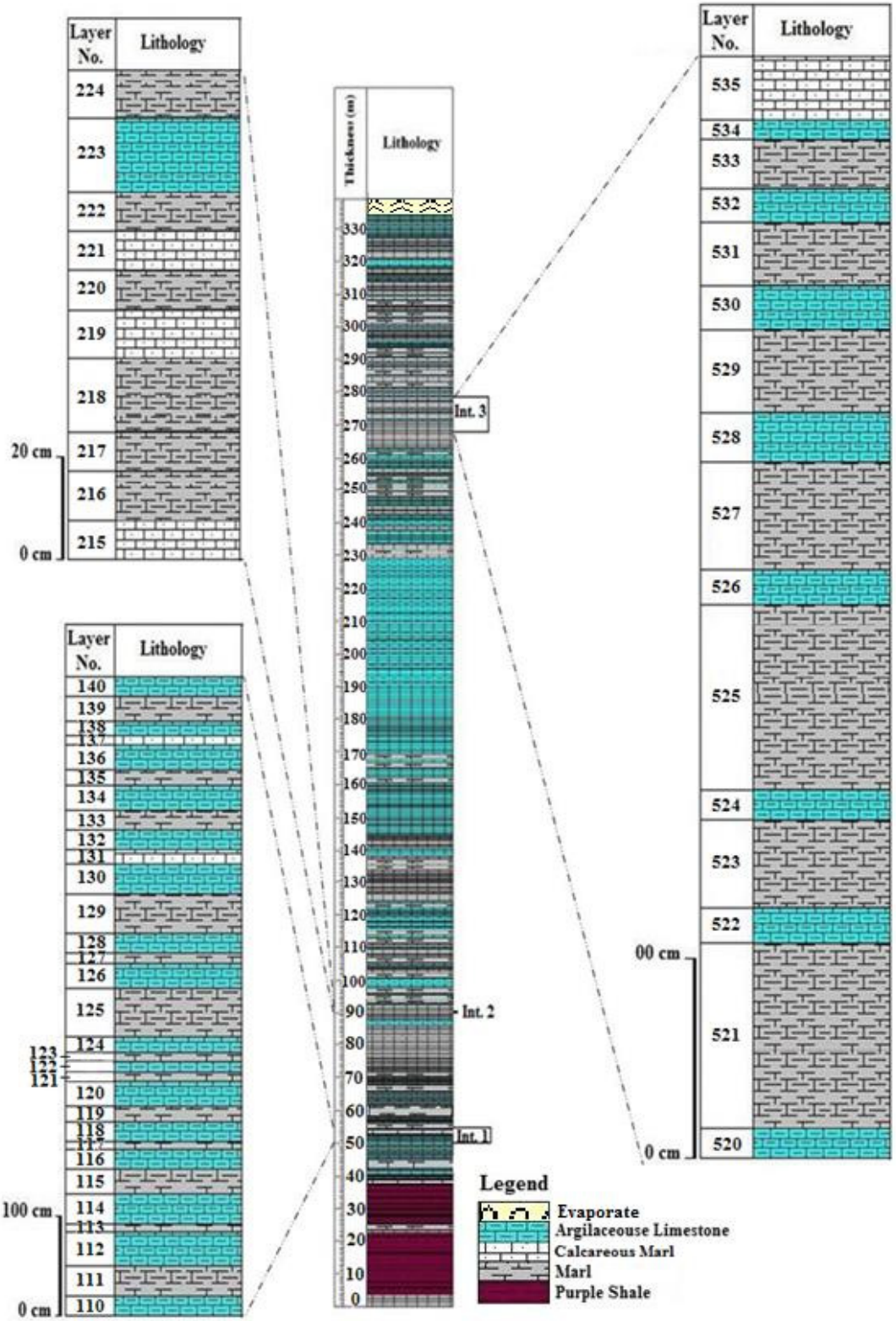

Figure 4. Lithological column of the studied section (see Fig.1 for location); three intervals are shown: interval 1(53–60m) consists of argillaceous limestone and marl, interval 2 (93–94m) consists of calcareous marl and marl and interval 3 (272–282m) consists of argillaceous limestone and marl rhythmites.

Materials and methods

Some 57 samples were selected from these three rhythmic intervals (31, 10 and 16 samples from the intervals 1, 2 and 3, respectively). A bed–by–bed analysis (geochemical analysis and microscopic investigations) of the rhythmites was performed. Microscopic investigations using polarizing microscope (Zeiss, Axioscope, 40) were done on thin sections which were prepared from the three interval samples. Scanning electron microscopy investigation using SEM (JEOl, JSM–840A) at the Faculty of Arts and Architecture, Bu–Ali Sina University, Hamedan, Iran, were performed on 5 samples coated with gold (*sensu* Eldrett *et al.,* 2015). XRD analysis was carried on 8 whole–rock samples. The carbonate content (expressed as $CaCO_3$%) which were determined through titration method (Carver, 1971). The organic matter content was determined via wet chemical oxidation (by H_2O_2) (after Lewis & McConchie, 1994). Element composition was measured by S4 Explorer/ x–ray Spectrometry–Bruker (WD XRF) in XRF analysis laboratory at Yazd University. Stable ^{13}C and ^{18}O isotopes by IRMS at McGill University, Montreal Canada were done on 57 bulk samples (Amberg *et al.,* 2016, Niebuhr & Joachimski, 2002). Carbon and oxygen isotope ratios were analyzed in dual inlet mode on a Nu Perspective isotope ratio mass spectrometer connected to a NuCarb carbonate preparation system. Approximately 80 μg of sample powder were weighed into glass vials and reacted individually with H_3PO_4 after heating to 90°C for 1 hour. The released CO_2 was collected cryogenically and isotope ratios were measured against an in–house reference gas in dual inlet mode. Samples were calibrated to VPDB (Vienna Pee Dee Belemnite) using house standards. Errors for both $\delta^{13}C$ and $\delta^{18}O$ were better than 0.05 (1σ) based on repeated analyses of standards. The nomenclatures of limestone, calcareous marl and marl are based on Dunham, 1962 and Pettijohn, 1987 respectively.

Results

Field observations

During field observations "calcareous marl", "marl" and "limestone" layers were recognized in a descriptive sense, i.e. more weathering–resistant limestone layers versus erosive interlayers. Individual limestone and marl/calcareous marl layers are relatively constant in thickness (rather than to be nodular in nature) and are laterally continuous over the width of the outcrop. No distinct difference was observed in colour between these rock types except for the marl layers in intervals 2 and 3. In interval 1, both limestone and marl layers display light–gray to medium light–gray colour. In intervals 2 and 3, limestone, calcareous marl layers have light–gray to medium light–gray colour, whereas marl layers show dark–gray colour. The thickness of individual marl/calcareous marl and limestone layers differs along the succession irregularly. In the interval 1, the thickness of marl layers is between 8–50cm and the thickness of limestone layers is 10–35cm. In the interval 2, the thickness of marl and calcareous marl layers is between 8–15cm and in the interval 3, the thickness of marl layers is between 50–190cm and the thickness of limestone layers varies from 20 to 50cm. The Gandab section comprises a suite of trace fossils that fall generally within the *Zoophycos* ichnofacies of Seilacher (1967). These include *Thalassinoides*, *Rhizocorallium, Planolites*, *Chondrites*, *Spirophyton* and *Zoophycos*. These traces were observed exclusively in the limestones. Field observations made in this study indicate extensive lateral continuity of individual beds, sharp contact between various lithologies and planar geometry of individual beds (Table 1, Fig. 5, A – D).

Facies/lithofacies types

Microfacies and lithofacies types of the study rhythms include alternation of carbonate microfacies with marl lithofacies. Microfacies analyses of carbonate rocks were performed by light microscopy based on Dunham (1965) scheme. Facies and lithofacies characters were used to verify their depositional environments. Two microfacies were defined:

MF1 (Foraminifera Wackestone): This microfacies, consists of 10–20% bioclasts dispersed in a micritic matrix. The bioclasts include planktonic (*Globigerinidea* and *Globorotalidae*) and benthic foraminifera (*Lenticulina* and *Rotalidae*) and occasional bivalve clast (Fig. 6, A and B). In some parts of the section, this microfossils usually display crude/ and parallel–lamination (Fig. 7, A – F).

MF2 (Foraminifera Mudstone): This microfacies comprises 4–7% bioclasts including mostly benthic foraminifera and echinoderm and brachiopod, bivalve fragments and rare planktonic foraminifera.

Lithofacies 1: This lithofacies consists of marl layers containing both planktonic and benthic foraminifera bioclasts. It alternates with MF1.

Lithofacies 2: This lithofacies consists of marl layers with benthic foraminifera, echinoderm and brachiopod as well as quartz grains 4–11% (Fig. 6, C – E). It alternates with MF2.

SEM and XRD investigations

Scanning electron microscopy (SEM) and polarizing microscopy were used for petrography. Compaction, dissolution of constituents was determined qualitatively in microscopic investigation (Fig.8). Both limestone and marl/calcareous marl layers contain similar constituents such as calcareous microfossils (Fig.8, A and B). Allochems in all lithologies (limestone, marl and calcareous marl) don't show signature of compaction, flatting or bending (Fig. 8, A and B). All lithologies contain similar clay mineral (mostly illite, recognized by XRD analysis) (Fig. 8, C and D) and framboidal pyrite (Fig. 8, E and F).

Geochemical analysis

Calcium carbonate and organic matter content

The carbonate content, in interval 1, for carbonate–rich layers (limestone) is 75–83.5% and for carbonate–poor layers (marl and calcareous marl) is 50–70%. In interval 2, for carbonate–rich layers (calcareous marl) and carbonate–poor layers (marl) it is 65–71% and 40–55%, respectively. In interval 3, for carbonate–rich layers (limestone) and for carbonate–poor layers (marl and calcareous marl) it is 81–93% and 48–73%, respectively.

Table 1. Summary of the evidences of the primary rhythms in the study rhythmites

Interval 3	Interval 2	Interval 1		
+	+	+	extensive lateral continuity of individual beds References: Colombie, *et al.,* 2012, Vleeschouwer, *et al.,* 2013	**Field observation**
+	+	+	Sharp contact between different lithologies References: Cleaveland, *et al.,* 2002; Vecke, *et al.,* 2008; Vleeschouwer, *et al.,* 2013	
+	+	+	Planar geometry of individual beds References: Munnecke & Westphal, 2005; Amberg, *et al.,* 2016	
+	+	+	co–existence benthic foraminifera and planktonic foraminifera References: Westphal, *et al.,* 2004, Colombie, *et al.,* 2012	**Sedimentological and mineralogical studies**
–	–	+	oriented allochems References: Westphal, *et al.,* 2004, Colombie, *et al.,* 2012	
+	+	+	co–existence of broken allochems and planktonic foraminifera References: Westphal, *et al.,* 2004, Colombie, *et al.,* 2012	
+	+	+	Existence of similar clay mineral (mostly illite) in both of intercalated lithologies References: Westphal, *et al.,* 2004, Colombie, *et al.,* 2012	
+	+	+	Existence of detrital quarts grains) in both of intercalated lithologies References: Westphal, *et al.,* 2004, Colombie, *et al.,* 2012	
–	–	+	the plot of Al_2O_3 and SiO_2 against of TiO_2 analysis show different trend lines for limestone and marl References: Amberg, *et al.,* 2016	**Geochemical analysis**
–	–	–	The stable isotope data show systematic difference between intercalated lithologies References: Westphal, *et al.,* 2010, Amberg, *et al.,* 2016	

The + and – signs imply to existence (+) or lack (–) of evidence in the study intervals.

Figure 5. The field view of A) alternation of limestone and marl (interval 1), B) lateral bed continuity of the alternation (interval 1), C) alternation of calcareous marl and marl (interval 2), D) alternation of limestone and marl (interval 3).

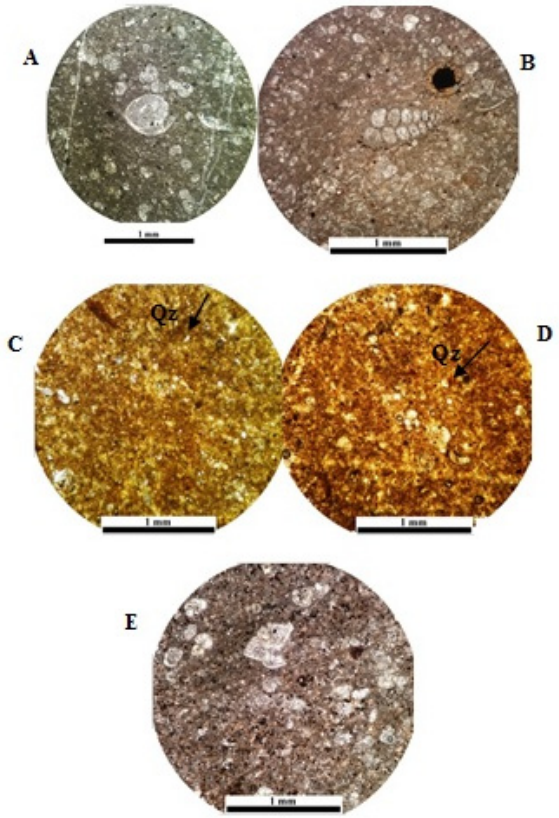

Figure 6. Photomicrographs of microfacies and lithofacies types: A and B, foraminifera wackestone; C, D, marl lithofacies and E, fossiliferous marl lithofacies.

In the intervals 1– 3, the organic matter mean content (wt. %) for the limestone and calcareous marl layers is less than the marl layers. The minimum, maximum and mean values are reported in Table 2. Fig. 9, shows box plot of these values for the three intervals.

Element composition (XRF)

In all of the three intervals, the SiO_2 and Al_2O_3/TiO_2 data were plotted and their corresponding trend lines were drown (Fig. 10, A–C). The Al_2O_3 mean content (wt.%) in interval 1, for limestone samples is 4.88 and for marl samples is 8.96, in interval 2, for calcareous marl samples is 6.62 and for marl samples is 11.1 and in interval 3, for limestone samples is 9.32 and for marl samples is 13.36. The TiO_2 mean content (wt.%) in interval 1, for limestone samples is 0.31, for marl samples is 0.73, in interval 2, for calcareous marl samples is 0.31 and for marl samples is 0.56 and in interval 3, for limestone samples is 0.54 and for marl samples is 0.84. The SiO_2 mean content (wt.%) in interval 1, for limestone samples is 49.23 and for marl samples is 51.15, in interval 2, for calcareous marl samples is 53.42 and for marl samples is 53.86 and in interval 3, for limestone samples is 32.83 and for marl samples is 43.4. The mean Al_2O_3/TiO_2 ratio in interval 1, for limestone samples is 15.97 and for marl samples is 12.52, in interval 2, for calcareous marl samples is 21.68 and for marl samples is 20.28 and in interval 3, for limestone samples is 17.37 and for marl samples is 15.97.

Table 2. The Minimum, maximum and mean values of organic matter and calcium carbonate in the study intervals

	Number of sample	Lithology		Min	Max	Mean
Interval 1	16	Limestone	$CaCO_3$ (%)	75	83	78.39
			Organic Matter (%)	0.99	4.18	2.85
	15	Marl	$CaCO_3$ (%)	50.5	69.25	59.18
			Organic Matter (%)	2.81	7	5.51
Interval 2	5	Calcareous marl	$CaCO_3$ (%)	52	71.25	64.1
			Organic Matter (%)	1.17	3.82	2.46
	5	Marl	$CaCO_3$ (%)	40.25	65.5	51.45
			Organic Matter (%)	0.62	2.61	1.8
Interval 3	8	Limestone	$CaCO_3$ (%)	81.25	93.25	88.1
			Organic Matter (%)	2.32	3.79	3.18
	7	Marl	$CaCO_3$ (%)	48.75	66.25	58.82
			Organic Matter (%)	2.97	5.65	4.1

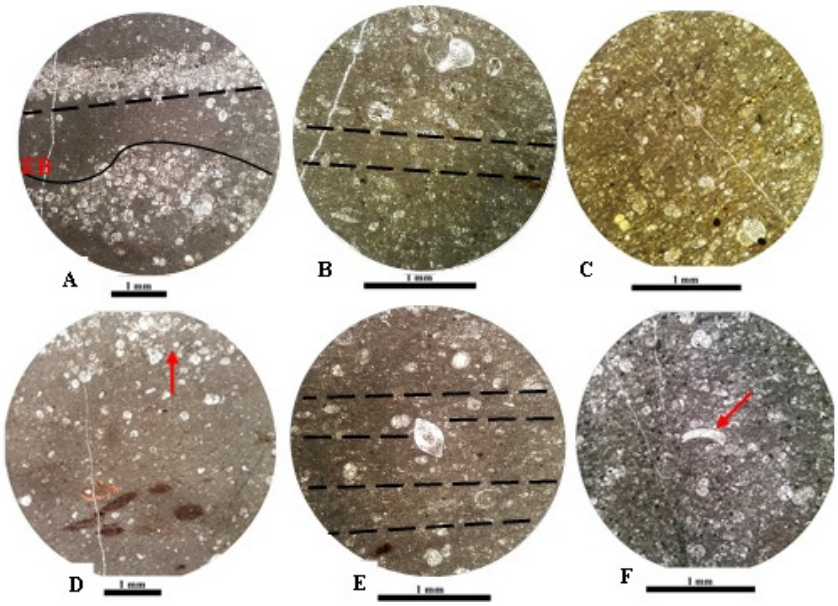

Figure 7. Photomicrographs of evidences of the current alignment of allochems: A, oriented microfossils and erosional base (EB) (alternation of mudstone and wackestone/packstone facies). B and C, crud lamination (wackestone facies). D, inverse grading (arrow) (wackestone facies). E, Benthic foraminifera and crud lamination (the arrow points the *Lenticulina*) (wackestone facies). F, broken allochem (arrow) (wackestone facies).

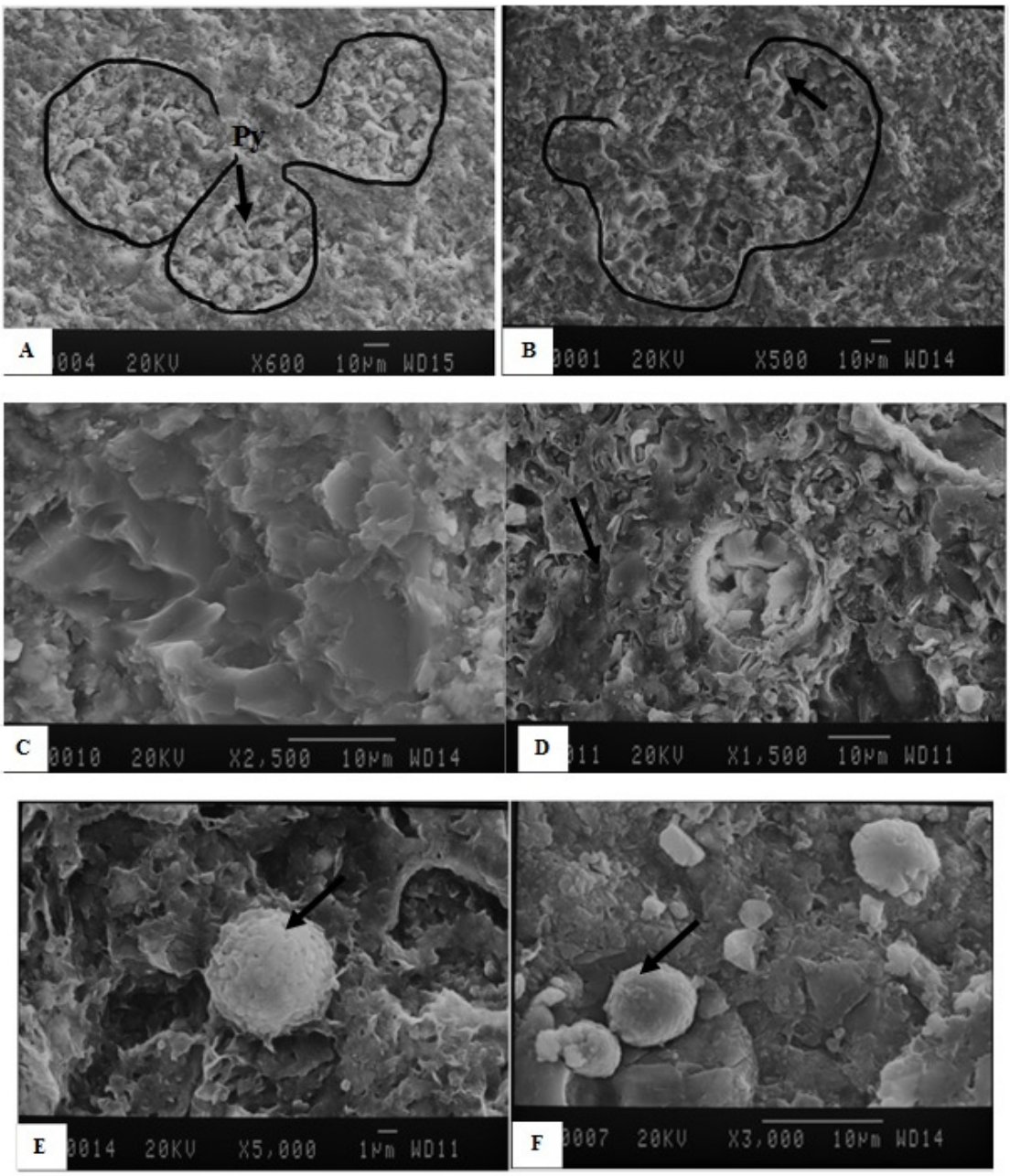

Figure 8. Scanning electron micrographs of various lithofacies types. A) three–chambered foraminifera with pyrite (py) filling (arrow) in a marl layer, B) foraminifera with microspar filling the chambers (arrow) in a limestone layer, C) clay mineral in limestone layer, D) clay mineral (arrow) in a marl layer, E) framboidal pyrite (arrow) in a marl layer, F) framboidal pyrite (arrow) in a limestone layer.

The mean SiO_2/TiO_2 ratio in interval 1, for limestone samples is 165.1 and for marl samples is 72.1, in interval 2, for calcareous marl samples is 162.34 and for marl samples is 113.1 and in interval 3, for limestone samples is 61.27 and for marl samples is 52.62. The ternary diagram of CaO, Al_2O_3 and SiO_2 (*sensu* Neuhuber & Wagreich, 2011) of the study samples shows the rhythmite lithologic composition in the study intervals (Fig. 11). The XRD analysis was carried on 8 whole–rock samples in order to identify the samples mineralogy (Table, 3). The results show similar mineralogy (quartz, calcite and illite) for all study samples.

Stable isotopes

The results of isotope analysis for the study intervals are as follow; in the interval 1, the

limestone samples have the oxygen isotope values range between –4.47 to –2.63 ‰ (mean= –3.86 ‰) and the carbon isotope values range +0.33 to +1 ‰ (mean = +0.54) and for the marl samples the oxygen isotope values range is between –4.27 to –3.08 ‰ (mean= –3.76 ‰) and the carbon isotope values range is between –0.98 to +0.42 ‰ (mean= –0.14 ‰). In the interval 2, the calcareous marl samples have the oxygen isotope values variy between –4.20 to –3.59 ‰ (mean= –3.93 ‰) and the carbon isotope values range +0.25 to +0.40 ‰ (mean= +0.34 ‰) and for the marl samples the oxygen isotope values vary between –4.22 to –3.82 ‰ (mean= –4.1 ‰) and the carbon isotope values range is +0.44 to +0.64 ‰ (mean= +0.51 ‰). In the interval 3, for the limestone samples the oxygen isotope values range is –1.83 to –1.01 ‰ (mean= –1.34 ‰) and the carbon isotope values range is between –3.53 to –1.17 ‰ (mean= –2.65 ‰) and for the marl samples the oxygen isotope values range is –5.68 to –1.87 ‰ (mean= –3.18 ‰), the carbon isotope values range is –2 to –0.45 ‰ (mean= –0.98 ‰).

Table 3. The results of mineralogy for the selected samples of the study rhythmites by XRD.

XRD	Sample No.	Mineralogy
Interval 1	122	calcite, quartz, iIllite
	123	calcite, quartz, illite, dolomite, clinochlore
Interval 2	218	calcite, quartz, illite – montmorilonite
	219	calcite, quartz, illite
	220	calcite, quartz, illite
Interval 3	520	calcite, quartz, illite
	521	calcite, quartz, illite
	533	calcite, quartz, illite

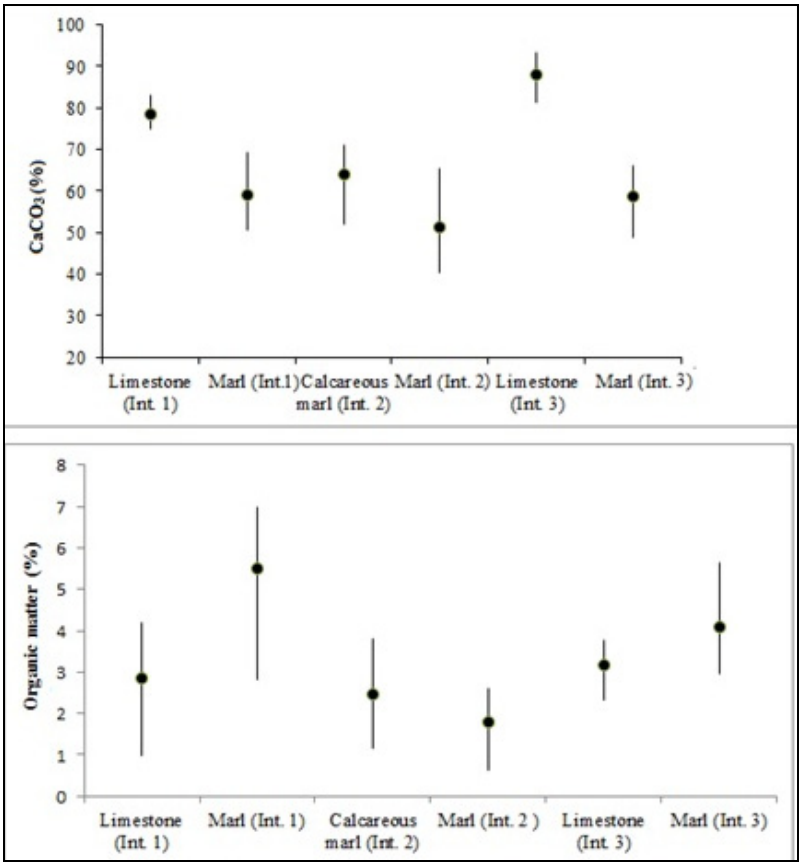

Figure 9. Box plot of organic matter and $CaCO_3$ content for the three intervals (Int.); maximum organic matter content is seen in marl samples, whereas maximum carbonate content is seen in limestone samples.

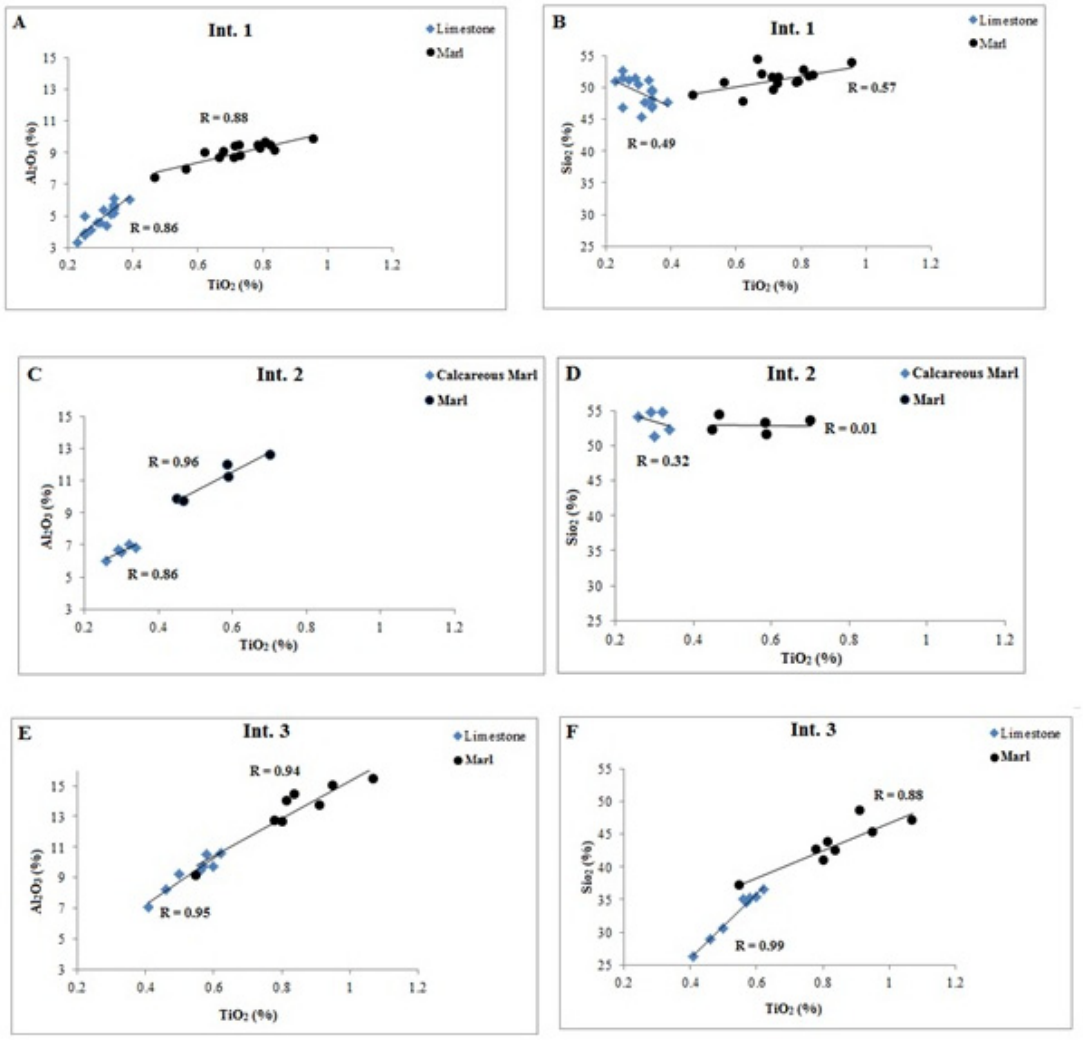

Figure 10. A–F cross plots of SiO_2/TiO_2 and Al_2O_3/TiO_2, from the intervals 1 to 3; A and B) interval 1: two distinct trend lines indicating a bimodal chemical composition and thus, varying environmental conditions (or depositional mechanism). B and C) interval 2, and E and F) interval 3: similarity of the most trend lines may imply that the precursor sediment of limestone layers and marls/ calcareous marl was identical.

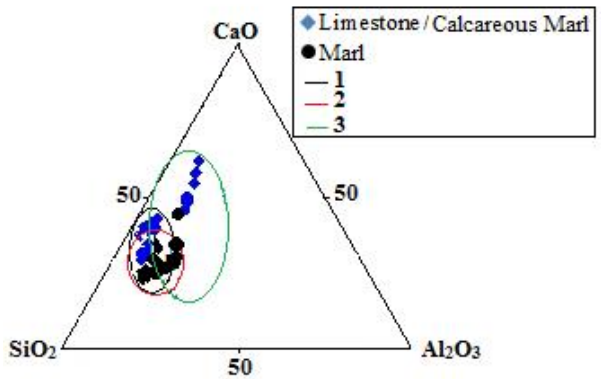

Figure 11. Ternary diagram of CaO, SiO_2 and Al_2O_3 (Wt.%) (*sensu* Neuhuber & Wagreich, 2011) showing the intercalated lithologies element composition in the study intervals; 1, 2 and 3 for intervals 1 to 3, respectively.

In the interval 1, the similar depletion (in compare with Eocene marine calcite) in the oxygen isotope is observed in limestone and marl samples; whereas for the marl samples, the carbon isotope is more depleted. In the interval 2, both marl and limestone samples show similar depletion in oxygen and carbon isotopes. In the interval 3, the oxygen isotope values of marl samples show more depletion than limestones, whereas the limestone samples carbon isotope is the more depleted than marl samples. Generally, from interval 1 to interval 3, carbon isotope shift toward lighter values for both marl and limestone samples. Shift to the lighter oxygen isotope values (from interval 1 to 3) only occurs in marl samples, while limestone samples show enrichment in contrast.

Evaluation of diagenetic overprint

The most important diagenetic process includes recrystallization of calcite, cementation, stylolite and pyrite formation which is dispersed in matrix in all rock types of the study rhythmites (Fig. 12). Geochemical analyses of some trace elements including Fe, Mg, Mn, K and Sr (diagenetically mobile elements) enable to detect diagenetic imprint (Paz & Rossetti, 2006). Normally, Al_2O_3 is considered to be diagenetically immobile, hence the ratio of diagenetically mobile elements and their oxides compared to Al_2O_3 contents reveals diagenetic changes that overprinted possible primary differences which may originally existed between limestones and interlayers (marl in the study rhythms) (Westphal *et al.,* 2004). Cross plot of Fe_2O_3, MgO, MnO, K_2O and SrO versus Al_2O_3 were plotted (Figs. 13 to 15) to survey any possible evidence. Furthermore, carbon and oxygen isotope composition of all of the study samples were compared with Eocene marine calcite isotopic signature (Holail, 1994) (Fig. 16).

Discussion

Extensive lateral continuity of individual beds is an evidence supporting a primary origin for rhythmic alternations (Elrick & Hinnov, 2007; Colombie *et al.,* 2012; De Vleeschouwer *et al.,* 2013); because chemical gradients controlling cm–scale dissolution and solution transport would not likely remain consistent over such long distances (Elrick & Hinnov, 2007). Sharp contact between two lithologies (presence of different lithologies) are interpreted to be primary depositional features (Cleaveland *et al.,* 2002; Vecke *et al.,* 2008; De Vleeschouwer *et al.,* 2013); because these changes reflect repetitive variations in carbonate content, in response to changes in the water column and in the geochemical conditions at the sediment/water interface (De Vleeschouwer *et al.,* 2013).

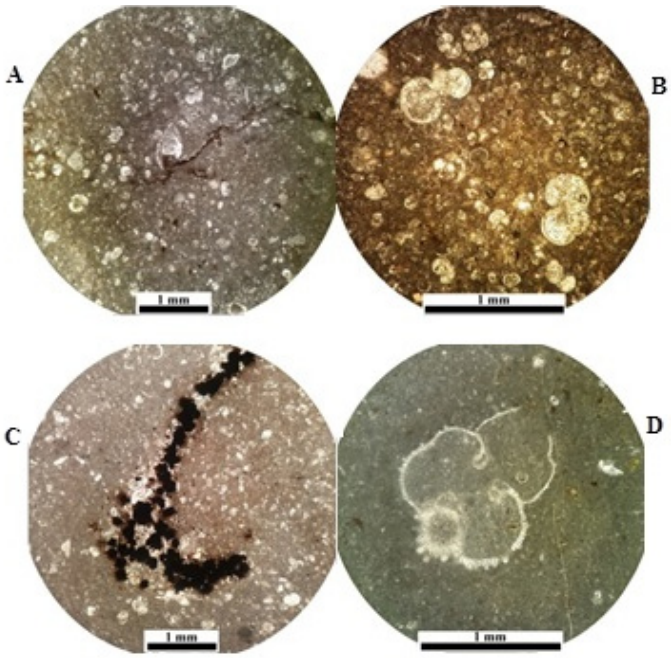

Figure 12. some of diagenetic properties in the study rhythmites; A) stylolite (wackestone facies), B) microfossils chambers with microspar filling (wackestone facies), C) Pyrite (mudstone/wackestone facies), D) micritization of foraminiferal chamber (mudstone facies).

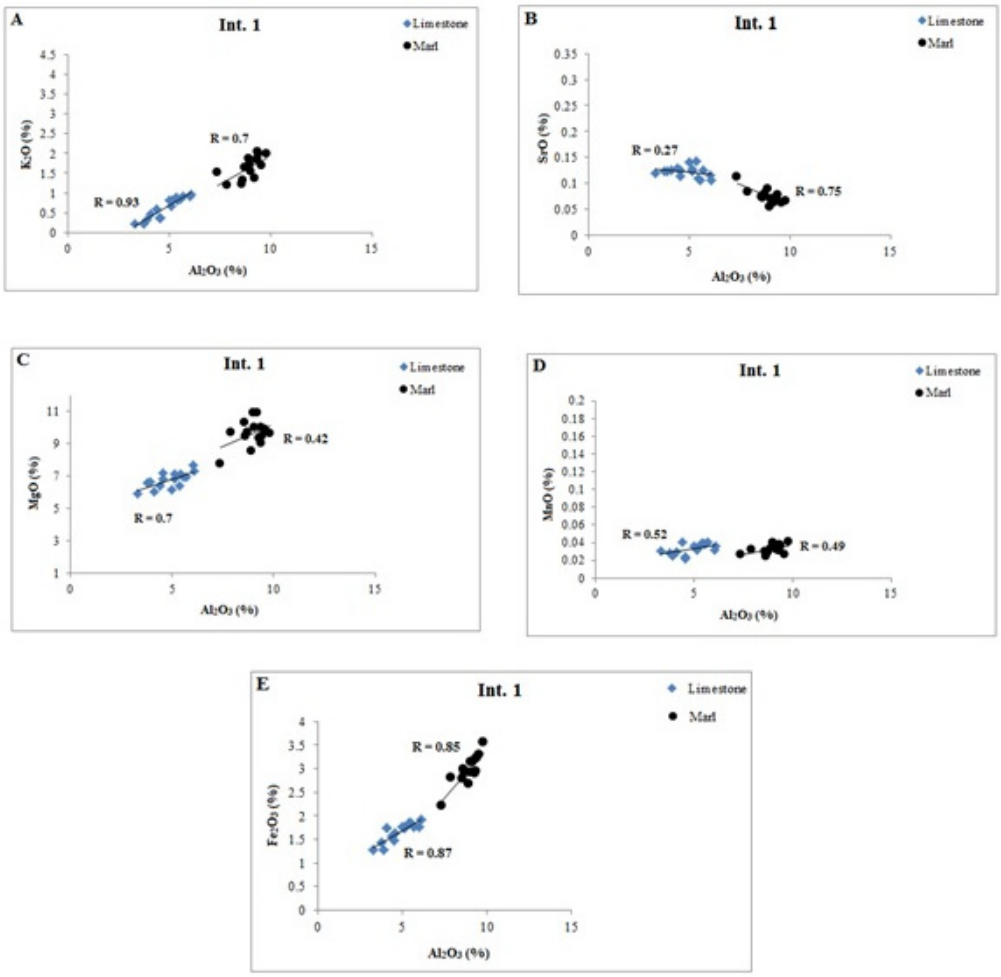

Figure 13. A–E cross plots of various trace elements vs. Al_2O_3, interval 1: most trace elements show strong correlation ($R \approx 0.7$) with Al_2O_3, indicating these samples were not affected by diagenesis, however a few elements (mainly MnO) show weak correlation ($R < 0.5$) with Al_2O_3.

Planar geometry of individual beds is useful for differentiating between primary and diagenetic calcareous rhythmites; diagenesis usually makes nodular morphology (Munnecke & Westphal, 2005; Amberg *et al.,* 2016). The trace fossils of *Zoophycos* group are normally associated with turbidites and debris flows in ramp environment. Frequent occurrences of such trace fossils in the study area could be assigned to event deposits (i.e. turbidite?).

Based on the type of microfacies, their vertical changes and the type of skeletal and non– skeletal components and comparison with the Flügel (2010), depositional environment of the study rhythmic alternation was proposed deep marine (outer–ramp and mid–ramp) (Fig. 17).

In MF1 (*Foraminifera Wackestone)*, presence of small whole fossil planktonic foraminifera as the main component associated by benthic foraminifera and micritic matrix indicates outer–ramp environment (below SWB). The microfacies is equivalent to RMF5 Flügel, 2010. Alternating marl and lime mud matrix rich in planktonic foraminifera was interpreted as outer–ramp environment (Geel, 2000; Amirshahkarami *et al.,* 2007).

In MF2, (*Foraminifera Mudstone),* dominant benthic foraminifera associated with shallow–water bioclasts such as echinoderm and brachiopod, planktonic foraminifera and micritic matrix indicates mid–ramp environment (Heckel, 1972; Amirshahkarami *et al.,* 2007). The microfacies is equivalent to RMF7 Flügel. Microfacies analysis of these rhythmites indicates the alternation of background in–situe sedimentation (carbonate facies) which was intermittently interrupted by fine clastics transported by traction currents from

shallow–marine that dumped siliciclastic into the deep–marine. Evidences such as micritic matrix, small planktonic foraminifera (i. e. *Globigerina* and *Globorotalia*) indicate deposition in calm deep–waters (Flügel, 2010) that were subject to events. This interpretation is supported by the presence of crud laminae, parallel lamination, and oriented fossil fragments (in the interval 1) and presence of the benthic foraminifera (*Rotalidea*), bivalve, brachiopod and echinoderm clasts as well as fine–sand quartz grain originated from shallow–water and transported by currents (probably represent distal turbidites?). Some characters of the rhythmites in the present study are similar to those reported by Eldrett *et al.,* (2015); i.e. in the limestone beds: 1) current alignments of fossils, 2) higher detritus materials and 3) lower organic carbon (OC) contents compared with marlstone beds. SEM investigations of the intercalated lithologies don't reveal different diagenetic pathways for the limestone and marl/calcareous marl layers. A prerequisite of the differential diagenesis model is that skeletal grains more undergone diagenetic process such as compaction and bending in marl interlayers than their limestone counterparts (Munnecke & Westphal, 2005). The results obtained from XRD analysis indicate that both of intercalated lithology have similar mineralogic content with no remarkable difference that decline a diagenetic differential scenario.

The fluctuation of the calcium carbonate content between limestone and marl layers can reflect productivity cycle (Seibold, 1952) and or dilution cycle (Einsele & Seilacher, 1982). The different organic matter content of the limestone and marl layers could be a sign of the different oceanic conditions (i.e. oxidation/deoxygenation) during the deposition of limestone and marl layers. Al_2O_3/TiO_2, SiO_2/TiO_2 plots are widely used for geochemical differentiation of rhythmite layers. For example, primary origin of the intercalated lithologies (bioturbated marl– laminated marl cycles) from the Trubi Formation (lower Pliocene; Punta di Maiata, Sicily) (Westphal *et al,* 2008) was distinguished using geochemical data, the two different marl types clearly show a bimodal distribution in their Al_2O_3/TiO_2 ratios.

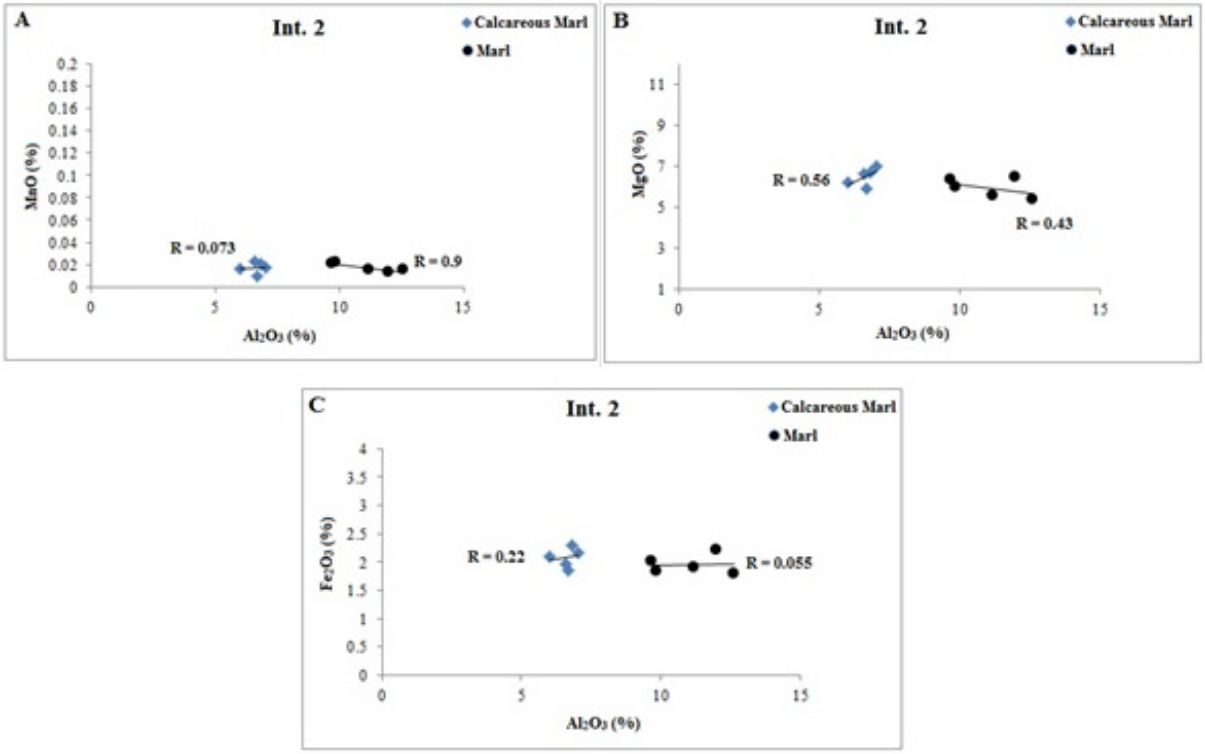

Figure 14. A–C cross plots of various trace elements vs. Al_2O_3, for the interval 2: most trace elements show weak–moderate correlation ($R < 0.56$) with Al_2O_3 which imply they were probably altered by diagenesis.

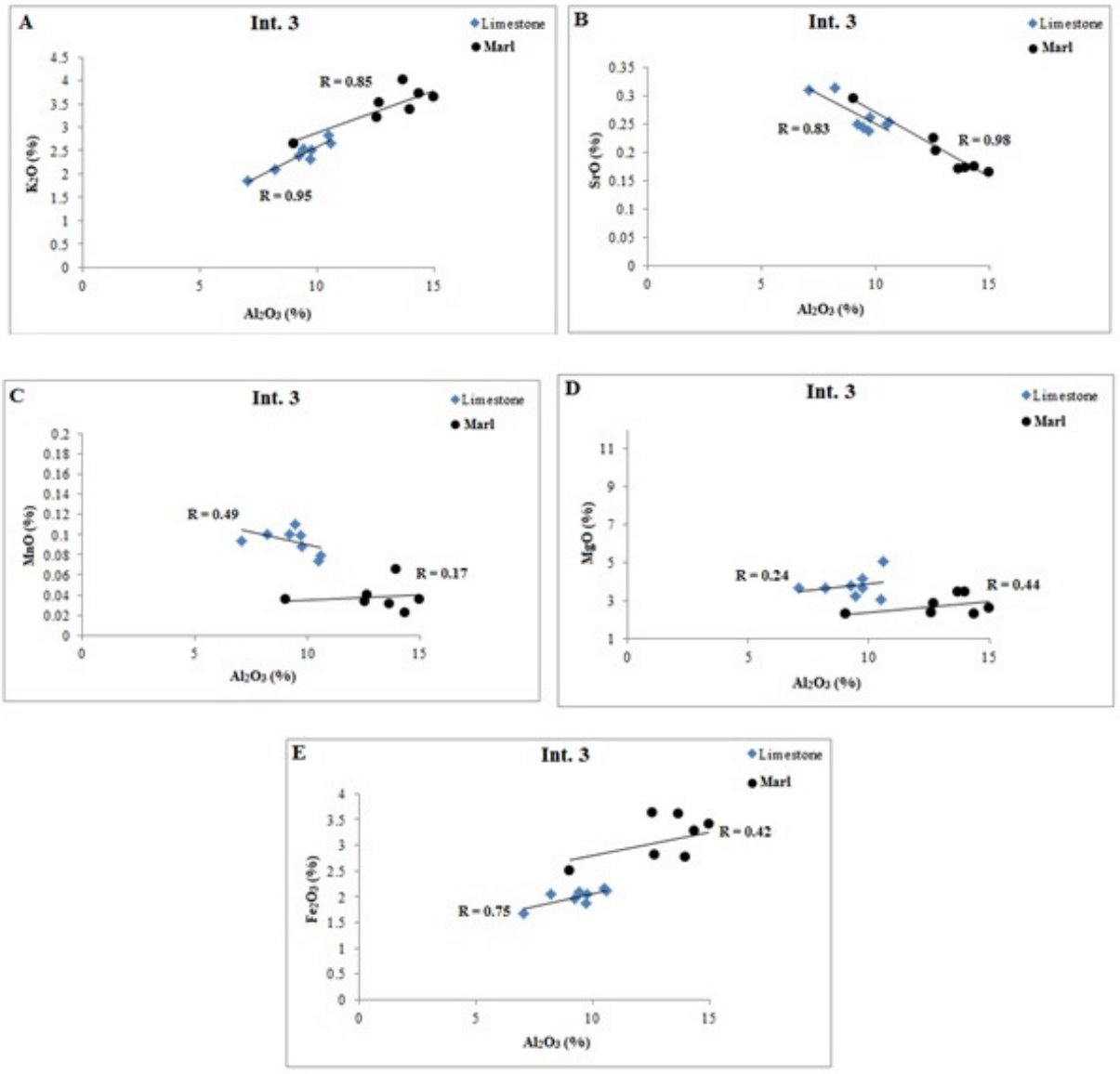

Figure 15. A–E cross plots of various trace elements vs. Al_2O_3, for the interval 3: there are weak correlation (R < 0.5) between MnO, MgO, Fe_2O_3 (for marl samples) and Al_2O_3 which may be due to diagenetic effect, however correlations between K_2O, SrO with Al_2O_3 are strong (R > 0.83).

Eldrett *et al.,* (2015) recognized the primary origin of limestone–marlstone cycles of the Cretaceous Western Interior Seaway, USA using Al_2O_3, TiO_2 and SiO_2 cross plots. However, cross plot of XRF results from Cretaceous pelagic limestone–marl alternations from the Blacke–Bahama Basin (Westphal *et al,* 2004) and Ordovician limestone–marl alternations in Oslo–Asker District Norway (Amberg *et al.,* 2016) show that high correlation coefficient of diagenetically rather stable elements (Si and Ti) with diagenetically stable element (Al) demonstrate that the precursor sediment was undifferentiated; and weak or negative correlation between diagenetically mobile elements and Al_2O_3 imply diagenetic changes. The two lithologies in the interval 1, clearly show separate trend lines (with strong correlation coefficient) and a bimodal chemical composition in Al_2O_3/TiO_2, SiO_2/TiO_2 plots (Figs. 10). Although, the bimodal distribution (population) is also observed in the Al_2O_3/TiO_2, SiO_2/TiO_2 plots of intervals 2 and 3 (Figs. 10), a pronounced difference with that of interval 1 is notable: the trend lines of two lithologies show

either linear or weak correlation (Fig. 10). This characterizes diagenetic overprint on a primary rhythm. Geochemical analysis (in bulk–rock samples) of mobile trace elements oxides (i.e. K_2O, MnO, Fe_2O_3 and SrO) compared to Al_2O_3 are also used as indicators of diagenetic alteration masked possible primary differences in rhythmites lithologies (Westphal *et al.,* 2004, Brand *et al.,* 2012). Similarity of the trend line and geochemical behavior of mobile elements vs. Al_2O_3 (as an immobile element during diagenesis) is used to evaluate diagenetic alteration (Westphal *et al.,* 2004). Such behavior is evident between K_2O, MgO, MnO and Fe_2O_3 vs. Al_2O_3 in the interval 1, which shows they were not strongly affected by diagenetic processes. This conclusion is supported by field observations and sedimentary structures in the study rhythms (Table 1). As a mobile element, manganese usually becomes enriched and strontium depleted during post–depositional dissolution and recrystallization of carbonate (Veizer, 1983; Ullmann *et al.,* 2013). In the study rhythmites, Sr decreases in the marl interlayers from interval 1 to 2; whereas Mn content increases in both limestone and marl interlayers from intervals 1 to 3 (compare MnO/Al_2O_3 and SrO/Al_2O_3 cross–plots in Figs. 13 through 15). These facts imply the study samples were somewhat affected by diagenesis and the variations that do exist in trace element concentration between intercalated lithologies could also reflect environmental perturbation such as the different sources of sediments (Swart & Oehlert, 2018). In contrast to the interval 1, although the intervals 2 and 3 show somewhat bimodal populations, the weak correlation (R = 0.5) between SrO, MgO, MnO and Fe_2O_3 vs. Al_2O_3 in these intervals (Figs. 13 and 15) may figure out possible diagenetic overprint on the nature of primary rhythm.

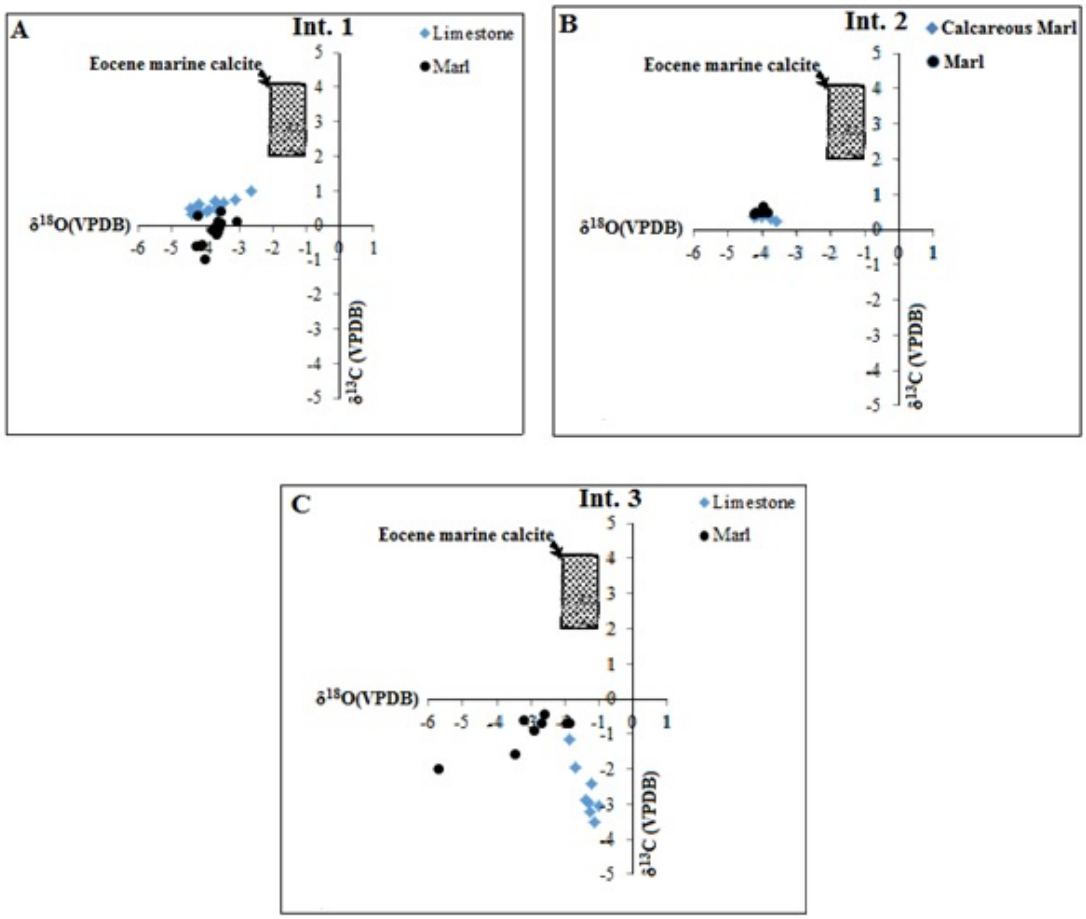

Figure 16. A–C carbon vs. oxygen stable isotope composition for the study three intervals (Int. = interval), there is deviation from Eocene marine calcite isotope composition (Holail, 1994) indicating diagenetic alteration.

Fluctuations in $\delta^{13}C$ values of early Cenozoic probably reflect cyclic oscillating oceanographic conditions. These oscillations may be related to: 1) the mean C isotopic composition of sea water, or 2) sea water productivity or nutrient levels (Bralower *et al.,* 1995). Depletion of $\delta^{13}C$ values (up to 2.7‰) in the Paleocene–Eocene marine sediments were reported by Zachos *et al.,* 1993; Thomas & Shakelton, 1995) which were related to the reduced carbonate production (=low sedimentation rate) or enhanced carbonate dissolution. Both ^{18}O and ^{13}C become progressively depleted during diagenesis (Thierstein *et al.,* 1991; Schobben *et al.,* 2016). Recrystallization is the most important non–biogenic process and mainly influences on ^{18}O composition. In contrast, biogenic processes such as OM oxidation or methane formation mainly control ^{13}C composition. As discussed above, diagenetic overprint is a main reason which complicates unraveling any possible original differences in rhythmites lithologies by geochemical analysis. However, the intensity of diagenesis can be recognized by stable isotope (i.e. ^{18}O and ^{13}C) analysis. Calcite is the main mineral in all the study intervals (Table 3) and its isotopic signature can be used to express the degree of alteration in whole rock samples. Reconstruction of the Eocene marine calcite isotopic composition (Holail, 1994) indicate the following isotopic composition (^{18}O = –1.0 to –2.0 ‰ and ^{13}C = +2.0 to +4.0 ‰). This composition may be significantly altered during diagenesis of which the most important processes are temperature variation, an (aerobic) OC oxidation, respectively (Schobben *et al.,* 2016), nutrient reduction and productivity reduction (Acıkalın *et al.,* 2015). Depletion up to 1 to 2‰ was reported due to these processes (Acıkalın *et al.,* 2015). The isotopic composition (O and C) of the interval 1 (limestone and marl rhythm) show moderate depletion (≈ 1 to 2‰) compared to the Eocene marine calcite (Fig. 17). The isotopic composition of the interval 2 (calcareous marl and marl rhythm) is almost similar to that of the interval 1 (Fig. 17). A distinct depletion is observed in the isotopic records of the interval 3 (^{18}O = –1.01 to –5.68‰ and ^{13}C = –0.45 to –3.53‰). This depletion can be related to biogenic processes (i.e. nutrient reduction, productivity reduction and OC oxidation for O and C isotopes respectively). In addition, the OC content of the interval (both limestone and marl beds, Fig. 9) supports this interpretation. Similar interpretations were reported by Acıkalın *et al.,* (2015) for such depletions in the isotopic records. It is notable that other processes (variation of depositional environments and/or the influence of marine currents, (Paz & Rossetti, 2006; Li *et al.,* 2018) may also cause such variations. This depletion can be also, related to depositional condition changes, probably due to entry of shallow currents (Paz & Rossetti, 2006; Li *et al.,* 2018) which is supported by the evidences of current activity in the interval 1. The more depletion of carbon isotopes of the interval 3 samples can't be justified by organic matter oxidation due to the preservation of high organic matter and manganese content. A possible scenario for this depletion can be nutrients deficiency and carbonate productivity reduction that is well confirmed by the abundant mudstone facies in interval 3.

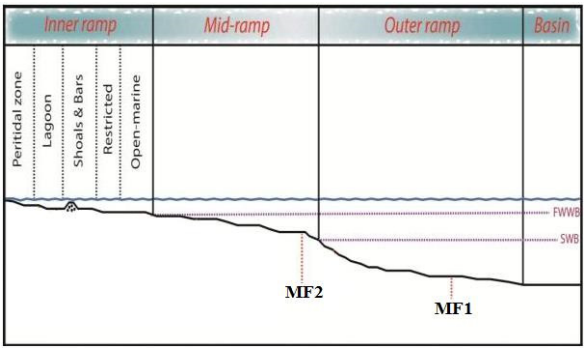

Figure 17. Proposed depositional environment model of rhythmic alternations of Pabdeh Formation.

Conclusions

This paper characterise rhythmical alternations between limestone and marls in Pabdeh Formation (Zagros Basin). Most marine rhythmites consist of alternating pelagic and hemipelagic sediments (i.e. carbonate–non carbonate couplets; Thierstein *et al.,* 1991; Eldrett *et al.,* 2015). The fact that two distinct lithologies alternate, suggests that the environmental conditions may have oscillated between two different modes (Westphal *et al.,* 2004). Results of Eldrett *et al.,* (2015) on the Cretaceous marl cycles of Western Interior Seaway (KWIS) of North America showed these cycles are due to variation of carbonate production (= times of limestone deposition) and OC production and preservation (= times of marlstone deposition); during the former periods the current intensity were also enhanced. These couplets reflect climatic forcing driven by insolation resulting from Milankovitch periodicities. The Eldrett *et al.,* (2015) model consists of two environmental

conditions: 1) times of limestone deposition (higher ventilation, higher intensity of currents and storms, more precipitation, higher carbonate production) and 2) times of marlstone deposition (mud rock deposition with enhanced stratification, higher OC production or preservation, weak currents and storms, redox condition).

The rhythmic succession in this study is composed of intercalated limestone, marl and calcareous marl layers. In general, our results show these rhythmites are formed as results of oscillation of depositional conditions: carbonate production, siliciclastic and terrestrial input. Subsequently, these rhythms were subjected to diagenetic alteration. Fluctuation in terrestrial influx resulting from the traction currents can be utilized as an explanation for the limestone–marl couplets, which is comparable to the dilution model (Westphal *et al.,* 2004). Such fluctuations in terrestrial influx are manifested by increase in siliciclastic material input during steady carbonate sedimentation and thereby formation of marls. This interpretation is supported by less microfossil content of the marl lithofacies (compared to the limestone beds, see the following). In the productivity model, significant variation in the microfossil content of the intercalated lithologies were proposed as a cause for the rhythmic deposits (Westphal *et al.,* 2004). In the study area (interval 1), there is significant difference in the microfossil content of the intercalated lithologies (10–20% and 4–7%, for limestone and marl layers, respectively).

Acknowledgements

We deeply appreciate our reviewers for the meticulous and instructing comments provided for the organization along with content of this paper. Logistics and sample preparations and geochemical analysis of this research were funded by grants to S. Khodabakhsh and H. Mohseni from vice President Research Affair of the Bu–Ali Sina University. Stable isotope analysis was funded by Gallen Halverson which is greatly acknowledged. Kindly assistants of Miss. E. Paseban and Mr. A. Hosseini, E. Hosseini, R. Zeybaram Javanmard, E. Heidari, Mr. Mehdizadeh during field trips is well acknowledged. Our acknowledge is also due to Prof. H. Westphal (Bremen University, Germany) whose valuable comments improved the manuscript quality. The authors thank Dr. B. Rafiei (Bu–Ali Sina University) for interpretation of XRD analysis.

References

Açıkalın, S., Ocakoğlu, F., Yılmaz, İ.Ö., Vonhof, H., Hakyemez, A., Smit, J., 2015. Stable isotopes and geochemistry of a Campanian–Maastrichtian pelagic succession, Mudurnu–Göynük Basin, NW Turkey: Implications for palaeoceanography, palaeoclimate and sea–level fluctuations. Palaeogeography, Palaeocli –matology, Palaeoecology, 441: 453–466.

Alavi, M., 2004. Regional stratigraphy of the Zagros fold thrust belt of Iran and its proforeland evolution. American Journal of Science, 304: 1–20.

Amberg, C.E.A., Collart, T., Salenbien, W., Egger, L.M., Munnecke, A., Nielsen, A.T., Monnet, C., Hammer, Q., Vandenbroucke,T.R.A., 2016. The nature of Ordovician limestone– marl alternations in the Oslo– Asker District (Norway): witnesses of primary glacio–eustasy or diagenetic rhythms? Scientific reports, 6:18787.

Amirshahkarami, M., Vaziri–Moghaddama, H., Taheri, A., 2007. Sedimentary facies and sequence stratigraphy of the Asmari Formation at Chaman–Bolbol, Zagros Basin, Iran. Journal of Asian Earth Sciences, 29: 947–959.

Arzani, N., 2004. Diagenetic evolution of mudstones: Black shales to laminated limestones, an example from the Lower Jurassic of SW Britain. Journal of Sciences, 15: 257–267.

Arzani, N., 2006. Primary versus diagenetic bedding in the limestone–marl/shale alternations of the epiric seas, an example from the Lower Lias (Early Jurassic) of SW Britain. Carbonates and Evaporates, 21: 94–109.

Bahroudi, A., Koyi, H.A., 2004. Tectono–sedimentary framework of the Gachsaran Formation in the Zagros foreland basin. Marine and Petroleum Geology, 21: 1295–1310.

Berberian, M., 1995. Master "blind" thrust faults hidden under the Zagros folds: active basement tectonics and surface morphotectonics. Tectonophysics, 24: 193–224.

Berberian, M., King, G.C.P., 1981. Toward a paleogeography and tectonic evolution of Iran. Canadian Journal of Earth Sciences, 18: 210–265.

Biernacka, J., Borysiuk, K., Raczyñski, P., 2005. Zechstein (Ca1) limestone–marl alternations from the North–Sudetic Basin, Poland: depositional or diagenetic rhythms? Geological Quarterly, 49. 1–14.

Bralower, T.J., Zachos, J.C., Thomas, E., Parrow, M., Paull, C.K., Kelly, D.C., Silva, I.P., Sliter, W.V., Lohmann, K.C., 1995. Late Paleocene to Eocene paleoceanography of the equatorial Pacific Ocean: Stable isotopes recorded at Ocean Drilling Program Site 865, Allison Guyot. Paleoceanography, 10: 841–865.

Brand, U., Jiang, G., Azmy, K., Bishop, J., Montanez, I.P., 2012. Diagenetic evaluation of a Pennsylvanian carbonate

succession (Bird Spring Formation, Arrow Canyon, Nevada, USA)–1: Brachiopod and whole rock comparison. Chemical Geology, 308: 26–39.

Carver, R.E., 1971. Procedures in sedimentary petrology. Wiley Interscience, 653 pp.

Cleaveland, L.C., Jensen, J., Goese, S., Bice, D.M., Montanari, A., 2002. Cyclostratigraphic analysis of pelagic carbonates at Monte dei Corvi (Ancona Italy) and astronomical correlation of the Serravallian– Tortonian boundary. Geology, 30: 931–934.

Collart, T., 2013. A potential paleo–environmental signal in the calcareous rhythmites of the Frognerkilen Formation (uppermost Sandbian – lower Katian) in Norway. Thesis of master degree, University Gent, Faculteit Wetenschappen Opleiding Master of Science in de geologie, P, 174.

Colombie, c., Schnyder, J., Carcel, D., 2012. Shallow–water marl–limestone alternations in the Late Jurassic of western France: Cycles, storm event deposits or both? Sedimentary Geology, 271–272: 28–43.

Dunham, R.J., 1965. Classification of carbonate rocks according to depositional texture: in: Ham, W.E. (ed.), Classification of Carbonate Rocks. AAPG, 1:108–121.

Einsele, G., Seilacher, A., (eds.), 1982. Cyclic and event stratification. Springer–Verlag, P. 540.

Eldrett, J.S., Ma, C., Bergman, S.C., Ozkan, A., Minisini, D., Lutz, B., Jackett, S.J., Macaulay, C., Kelly, A.E., 2015. Origin of limestone– marlstone cycles: Astronomic forcing of organic–rich sedimentary rocks from the Cenomanian to early Coniacian of the Cretaceous western interior Seaway, USA. Earth and Planetary science letters, 423: 98–113.

Elrick, M., Hinnov, L.A., 2007. Millennial–scale paleoclimate cycles recorded in widespread Palaeozoic deeper water rhythmites of North America. Palaeogeography, Palaeoclimatology, Palaeoecology, 243: 348–372.

Flügel, E., 2010. Microfacies of carbonate rocks: Analysis, Interpretation and Application. Springer – Verlag, Berlin Heidelberg New York, 924, pp.

Geel, T., 2000. Recognition of stratigraphic sequences in carbonate platform and slope deposites, Empirical model based on microfacies analysis of Paleogene deposits in southeastern Spain. Palaeogeography, Palaeoclimatology, Palaeoecology, 155: 211–238.

Holail, H., 1994. Diagenesis of the Middlle Eocene "Nummulite bank" of the Giza pyramids plateau, Egypt: petrologic and $^{18}O/^{16}O$ evidence. Qatar University Science, 14: 146–152.

James, G.A., Wynd, J.G., 1965. Stratigraphic nomenclature of the Iranian oil consortium agreement area. American AAPG Bulletin, 49: 2182–2245.

Khavari, M.P., Hadavi, F., Ghasemi–Nejad, E., 2014. Nannostratigraphy and paleoecology Pabdeh Formation in NW Zagros, Ilam section. Paleontology, 2: 149–164.

Khodabakhsh, S., Behbahani, R., Mohseni, H., 2009. Cyclic and event deposits in Pabdeh Formation, Western Iran. Damghan University, 2: 37–48.

Lewis, D.W., McConchie, D., 1994. Analytical sedimentology. Chapman and Hall, 197.

Li, J., Caia, Z., Chen, H., Cong, F., Wang, L., Wei, Q., Luo, Y., 2018. Influence of differential diagenesis on primary depositional signals in limestone–marl alternations: An example from Middle Permian marine successions, South China. Palaeogeography, Palaeoclimatology, Palaeoecology, 495: 139–151.

Mirzaee Mahmoodabadi, R., Massih, A, Saeedi, S., 2010. High resolution sequence stratigraphy and depositional environment of Pabdeh Formation in Dashte – Arjan Area (Shiraz, Fars, Zagros, Iran). World Academy of Science, Engineering and Technology, 4: 11–22.

Mohseni, H., Behbahani, R., Khodabakhsh, S., Atashmard, Z., 2011. Depositional environments and trace fossil assemblages in the Pabdeh Formation (Paleogene), Zagros Basin, lran. Geology Paleontology, Abh. 262: 59–77.

Motiei, H., 1993. Stratigraphy of Zagros, treatise on the geology of Iran: Geological Survey of Iran. 583 pp.

Mount, j.F., Ward, P., 1986. Origin of limestone/marl alternations in the Upper Maastrichtian of Zumaya, Spain. Sedimentary Petrology, 2: 228–236.

Munnecke, A., Samtleben, C., 1996. The formation of micritic limestones and the development of limestone–marl alternations in the Silurian of Gotland, Sweden. Facies, 34: 159–176.

Munnecke, A., Westphal, H., 2005. Variations in primary aragonite, calcite and clay in fine–grained calcareous rhythmites of Cambrian to Jurassic age–an environmental archive? Facies, 51: 592–607.

Munnecke, A., Westphal, H., Reijmer, J.J.G., Samtleben, C., 1997. Microspar development during early marine burial diagenesis: a comparison of Pliocene carbonates from the Bahamas with Silurian limestones from Gotland (Sweden). Sedimentology, 44: 977–990.

Neuhuber, S., Wagreich, M., 2011. Geochemistry of Cretaceous Oceanic Red Beds – A synthesis. Sedimentary Geology, 235: 72–78.

Niebuhr, B., Joachimski, M.M., 2002. Stable isotope and trace element geochemistry of Upper Cretaceous carbonates and belemnite rostra (Middle Campanian, north Germany). Geobios, 35: 51–64.

Paz, J.D.S., Rossetti, D.F., 2006. Paleohydrology of an Upper Aptian lacustrine system from northeastern Brazil: Integration of facies and isotopic geochemistry. Palaeogeography, Palaeoclimatology, Palaeoecology, 241: 247–266.

Pettijohn, F.J., Potter, P.E., Siever, R., 1987. Sand and Sandstone. New York, 628p.

Schobben, M., Ullmann, C,V., Leda, L., Korn, D., Struck, U., Reimold, W.U., Ghaderi, A., Algeo, T. J., Korte, C., 2016. Discerning primary versus diagenetic signals in carbonate carbon and oxygen isotope records: An example from the Permian–Triassic boundary of Iran. Chemical Geology, 422: 94–107.

Seibold, E., 1952. Chemische untersuchungen zur Bankung im unteren Malm Schwabens, N. Jahrb. Geology Palaontology, Abh., 95: 337–370.

Seilacher, A., 1967. Bathymetry of trace fossils. Mar. Geol., 5: 413–428.

Senemari, S., 2018. Investigation of the Pabdeh–Asmri transition based on calcareous nanofossils biostratigraphy, in NE Gurpi anticline, Khozestan Province. Stratigraphy and sedimentology researches, 1: 19–30. (in Persian)

Sepehr, M., Cosgrove, J.W., 2004. Structural framework of the Zagros Fold–Thrust Belt, Iran. Marine and Petroleum Geology, 21: 829–843.

Sluijs, A., Roij, L.V., Harrington, G.J., Schouten, S., Sessa, J.A., Levay, L.j., Reichart, G.J., Slomp, C.P., 2014. Warming, euxinia and sea level rise during the Paleocene–Eocene Thermal Maximum on the Gulf Coastal Plain: implications for ocean oxygenation and nutrient cycling. Climate of the past, 10: 1421–1439.

Stoneley, R., 1981. The Geology of the Kuh–e Dalneshin Area of Southern Iran, and Its Bearing on the Evolution of Southern Tethys. Journal of the Geological Society, London, 138: 509–526.

Swart, P.K., Oehlert, A.M., 2018. Revised interpretations of stable C and O patterns in carbonate rocks resulting from meteoric diagenesis. Sedimentary Geology, 364: 14–23.

Ullmann, C.V., Hesselbo, S.P., Korte, C., 2013. Tectonic forcing of Early to Middle Jurassic seawater Sr/Ca. Geology, 41: 1211–1214.

Veizer, J., 1983. Trace elements and isotopes in sedimentary carbonates. Reviews in mineralogy and geochemistry, 11: 265–299.

Vleeschouwer, D.D., Rakocinski, M., Racki, G., Bond, D.P.G., Sobien, K., Claeys, P., 2013. The astronomical rhythm of Late–Devonian climate change (Kowala section, Holy Cross Mountains, Poland). Earth and Planetary Science Letters, 365: 25–37.

Westphal, H., Head, M. J., Munnecke, A., 2000. Differential diagenesis of rhythmic limestone alternations supported by palynological evidence. Journal of Sedimentary Research, 70: 715–725.

Westphal, H., Munnecke, A., Bohm, F., Bornholdt, S., 2008. Limestone–marl alternations in epeiric sea settings – witnesses of environmental changes, or of rhythmic diagenesis? In: Holmden, C., Pratt, B. R., (eds.), Dynamics of Epeiric Seas: Sedimentological, Paleontological and Geochemical Perspectives. Geological Association of Canada Special Paper, 48: 389–406.

Westphal, H., Munnecke, A., Pross, J., Herrle, J.O., 2004. Multiproxy approach to understanding the origin of Cretaceous pelagic limestone–marl alternations (DSDP Site 391, Blake–Bahama Basin). Sedimentalogy, 51: 109–126.

Ziegler, M., 2001. Late Permian to Holocene paleofacies evolution of the Arabian plate and its hydrocarbon occurrences. GeoArabia, 6: 1–60.